PERGAMON

International Journal of Heat and Mass Transfer 43 (2000) 611–621

International Journal of HEAT and MASS TRANSFER

www.elsevier.com/locate/ijhmt

Free convection near a stagnation point in a porous medium resulting from an oscillatory wall temperature

J.H. Merkin[a,*], I. Pop[b]

[a]Department of Applied Mathematics, University of Leeds, Leeds LS2 9JT, UK
[b]Faculty of Mathematics, University of Cluj, R-3400 Cluj, CP 253, Romania

Received 7 February 1999

Abstract

A detailed theoretical study of unsteady free convection boundary-layer flow near the stagnation point of a two-dimensional cylindrical surface embedded in a fluid-saturated porous medium is presented when the surface temperature oscillates about a mean value above ambient. Both numerical and asymptotic solutions are employed to solve the governing equations for general values of the frequency ω and amplitude A of the surface temperature oscillations. Results for the heat transfer rate, boundary-layer thickness and temperature profiles are obtained for both small and large values of A and also for slow and fast oscillations. It is found that outside the thin boundary layer on the surface, a steady flow is induced for large times and fast oscillations. This steady boundary-layer flow is studied in detail for large values of the amplitude A.

1. Introduction

The role of convective flows in fluid-saturated porous media is now widely recognised to have important consequences in a wide range of applications as varied as geothermal flows, fibre and granular insulation and catalytic reactors. Several excellent books and review articles by Bejan [1], Nakayama [2], Kimura et al. [3], Nield and Bejan [4] and Ingham and Pop [5] have appeared recently dealing with this area, which review the present understanding of the basic mechanisms involved as well as showing how these impinge on the practical applications. One of the most fundamental components of models of convection in porous media is the flow, usually at high Rayleigh number, near an impermeable surface generated by differences in temperature between the surface and the surrounding medium. Various sorts of surface conditions have been considered, including prescribed temperature and prescribed rates of heating and, more recently, the heating resulting from a catalytic surface reaction [6–8]. Both steady-state configurations as well as the transient development of these flows have been extensively treated, the details are provided in Refs. [1–5], for example.

These previous studies, while they have produced many clear insights into the basic processes, have almost invariably been concerned with temporally constant surface conditions. It is not always the case that the maintenance of such constant conditions is a realistic assumption; often there are fluctuations about some mean value. The influence of temporal oscillations in surface conditions on convective flows in porous media has received very little attention to date. The purpose of the present paper is to make a start on trying to understand this feature by treating a rela-

* Corresponding author. Tel.: +44-113-243-1751; fax: +44-113-233-5108.

E-mail addresses: amtjhm@amsta.leeds.ac.uk (J.H. Merkin), popi@math.ubbcluj.ro (I. Pop)

0017-9310/00/$ - see front matter
PII: S0017-9310(99)00152-0

Nomenclature

A	amplitude of the surface temperature oscillations
f	reduced stream function
g	acceleration due to gravity
K	permeability of the porous medium
l	length scale
Q	heat transfer rate
Ra	Rayleigh number
$S(x)$	shape function
t	time
T	fluid temperature
T_w	mean surface temperature
T_∞	ambient fluid temperature
ΔT	temperature scale
u, v	velocity components in the x- and y-directions, respectively
U_0	velocity scale
x, y	Cartesian co-ordinates along the cylindrical surface and normal to it, respectively
α	effective thermal diffusivity
β	thermal expansion coefficient
τ	reduced dimensionless time
θ	dimensionless temperature
ν	kinematic viscosity
δ_1	boundary-layer thickness
σ	ratio of composite material heat capacity to convective fluid heat capacity
ψ	stream function
ω	frequency of surface temperature oscillations

Superscripts

$'$	differentiation with respect to y or $\tilde{y}$
$\bar{}$	dimensionless variables

tively simple, though basic, model problem. We consider the high Rayleigh number (boundary-layer) natural convection flow near a two-dimensional stagnation point (thus allowing the governing equations to be simplified) and take sinusoidal oscillations in the prescribed surface temperature about some mean value T_w which is above the ambient temperature T_∞ of the surrounding medium. We examine the effect of the amplitude and frequency of these surface temperature oscillations on the structure of the flow, obtaining asymptotic approximations for small amplitudes and for both fast and slow oscillation modes. We complement these analytic results with numerical simulations of the full problem for parameter values not amenable to asymptotic analysis. This leads us to find that there is a maximum amplitude of the oscillations about T_w for which a stagnation-point flow is possible with this maximum amplitude being strongly dependent on the frequency of the oscillations, decreasing as the frequency increases.

The physical situation considered in the present paper is easily amenable to experiment and merits consideration because of its possible application in automatic control systems in porous media. A good example of this model is the case of the physically realistic boundary condition of mean uniform surface heat flux, which is known to produce non-uniform surface temperatures. We note to this end that the first papers to study the effects of temperature oscillations on free convection boundary layers in a Newtonian (clear) fluid are those of Merkin [9], Kelleher and Wang [10] and Brown and Riley [11]. The latter authors discussed the problem of free convection over a vertical semi-infinite flat plate in a viscous (non-porous) fluid with a prescribed dimensionless temperature distribution of the form $1+\epsilon\exp(i\omega t)$, where $\epsilon \ll 1$, obtaining both numerical and asymptotic solutions using $(\omega\xi)$ as a parameter, where $\xi = x^{1/2}$ and x being the dimensionless co-ordinate along the plate. They found reasonable agreement between the numerically computed and asymptotic (for $\omega\xi$ large) values of the disturbance heat transfer. The phase settled down to its predicted value when $\omega\xi \simeq 7$ whereas agreement between the amplitudes required the somewhat higher values of $\omega\xi \simeq 15$.

2. Equations

We assume that Darcy's law is valid to describe the flow within the porous medium, which we take to be isotropic and homogeneous. If we also assume that the Boussinesq approximation holds, then the equations which govern the high Rayleigh number, unsteady convective flow (boundary-layer equations) near a cylindrical surface are, from Merkin and Mahmood [7] and Nield and Bejan [4], for example,

$$\frac{\partial u}{\partial x} + \frac{\partial v}{\partial y} = 0 \tag{1}$$

$$u = \frac{gK\beta}{\nu}(T - T_\infty)S(x) \tag{2}$$

$$\sigma\frac{\partial T}{\partial t}+u\frac{\partial T}{\partial x}+v\frac{\partial T}{\partial y}=\alpha\frac{\partial^2 T}{\partial y^2} \tag{3}$$

We solve Eqs. (1)–(3) subjected to the boundary conditions

$$\begin{aligned} &v=0,\ T=T_\infty+\Delta T(1+A\sin\omega t)\ \text{ on }\ y=0,\\ &T\to T_\infty\ \text{ as }\ y\to\infty\quad (t>0)\end{aligned} \tag{4}$$

$$u=v=0,\ T=T_\infty\ \text{ at }\ t=0\quad (x,\ y>0) \tag{5}$$

where u and v are the velocity components (as given by Darcy's law) in the x- and y-directions, respectively, with x and y being co-ordinates measuring distance along and normal to the body surface, t is time, α is the equivalent thermal diffusivity, ν the kinematic viscosity of the convective fluid, σ the heat capacity ratio, K the permeability, β the coefficient of thermal expansion. $\Delta T=T_w-T_\infty$ is some temperature scale, and ω is the frequency and A the amplitude of the surface temperature oscillations. $S(x)=\sin\phi$, where ϕ is the angle between the outward normal from the body surface and the downward vertical. For our model of a two-dimensional stagnation-point flow, we have

$$S(x)=\frac{x}{l}, \tag{6}$$

where l is some length scale. We make Eqs. (1)–(5) dimensionless using a velocity scale

$$U_0=\frac{g\beta K\Delta T}{\nu}, \tag{7}$$

with Rayleigh number $Ra=g\beta K\Delta Tl/\nu\alpha$ and then writing

$$\begin{aligned} &u=U_0\bar{u},\quad v=U_0Ra^{-1/2}\bar{v},\quad \bar{x}=\frac{x}{l},\\ &\bar{y}=Ra^{1/2}\frac{y}{l},\quad \bar{t}=\frac{U_0}{\sigma l}t,\quad \bar{\omega}=\frac{\sigma l}{U_0}\omega,\\ &\theta=\frac{(T-T_\infty)}{\Delta T}\end{aligned} \tag{8}$$

This leads to the equations, on using Eq. (6) and dropping the bars for convenience,

$$\frac{\partial u}{\partial x}+\frac{\partial v}{\partial y}=0 \tag{9}$$

$$u=x\theta \tag{10}$$

$$\frac{\partial \theta}{\partial t}+u\frac{\partial \theta}{\partial x}+v\frac{\partial \theta}{\partial y}=\frac{\partial^2 \theta}{\partial y^2} \tag{11}$$

We can combine Eqs. (9) and (11) by writing

$$\psi=xf(y,\ t),\qquad \theta=\theta(y,\ t) \tag{12}$$

where ψ is the stream function which is defined in the usual way, namely $u=\partial\psi/\partial y$, $v=-\partial\psi/\partial x$, to give $\theta=\partial f/\partial y$. This leads finally to the equation for our model of stagnation-point flow as

$$\frac{\partial^3 f}{\partial y^3}+f\frac{\partial^2 f}{\partial y^2}=\frac{\partial^2 f}{\partial y\,\partial t} \tag{13}$$

with boundary and initial conditions (4) and (5) becoming

$$\begin{aligned} &f=0,\ \frac{\partial f}{\partial y}=1+A\sin\omega t\ \text{ on }\ y=0,\\ &\frac{\partial f}{\partial y}\to 0,\ \text{as}\ y\to\infty\quad (t>0)\\ &f=0\ \text{ at }\ t=0\quad (y>0)\end{aligned} \tag{14}$$

We note that, without any loss in generality, we need only consider the case $A\geq 0$.

We characterise our solution in terms of a surface heating (dimensionless) Q and a boundary-layer thickness δ_1 defined by

$$\begin{aligned} &Q=-\left(\frac{\partial\theta}{\partial y}\right)_{y=0}=-\left(\frac{\partial^2 f}{\partial y^2}\right)_{y=0},\\ &\delta_1=\int_0^\infty u\,\mathrm{d}y=f(\infty,\ t)\end{aligned} \tag{15}$$

3. Solution

The initial development of the solution follows the usual form for impulsively heated surfaces, giving, see Ref. [12],

$$\begin{aligned} &Q\sim\frac{1}{\sqrt{\pi}}t^{-1/2}+\cdots,\\ &\delta_1\sim\frac{2}{\sqrt{\pi}}t^{1/2}+\cdots\quad \text{for small}\ t\end{aligned} \tag{16}$$

The details are straightforward and are not of particular interest for our present purposes. We are concerned here with determining the behaviour of the solution for large times, for which Eqs. (13) and (14) have to be solved numerically for general values of the parameters A and ω. This can easily be achieved using standard methods [13,14]. We give results for three representative cases in Fig. 1, namely $A=0.2$, $\omega=1.0$; $A=0.4$, $\omega=0.25$ and $A=0.5$, $\omega=4.0$. In all the three cases the ultimate response is oscillatory with the same frequency as the applied wall temperature, though slightly out of phase with it. Q attains its maximum/minimum values before the corresponding turning points in the wall temperature, whereas δ_1 attains these values slightly afterwards. The amplitude of the response increases with A (as would be expected) with the amplitude being dependent on ω. For Q we find that the larger the value of ω (the faster the oscillations) the larger the amplitude for a given value of A. Negative values of Q are possible for sufficiently large values of A (see Fig. 1(c)). For δ_1 the opposite holds, with the larger responses being seen as ω is decreased (slower oscillations). A further feature to note is that the oscillations in Q and δ_1 are about a mean value which is above (for Q) and below (for δ_1) the steady ($A = 0$) case (for which $Q = 0.6276$ and $\delta_1 = 1.143$). This effect increases with A for a given frequency.

As A is increased a value is reached (dependent on ω) at which the solution breaks down. In these cases we find that there is still an oscillatory response (with the same frequency as the wall temperature) in a region close to the wall. However, now the boundary layer thickens (relatively quickly) with t and a situation is reached where the outer boundary condition is no longer satisfied by the numerical solution. Increasing sizes of spatial domain were tried in these computations and, in each case, the boundary layer thickness was seen to keep increasing with t. This point will be addressed in a little more detail below.

Further insights into the nature of the solution can

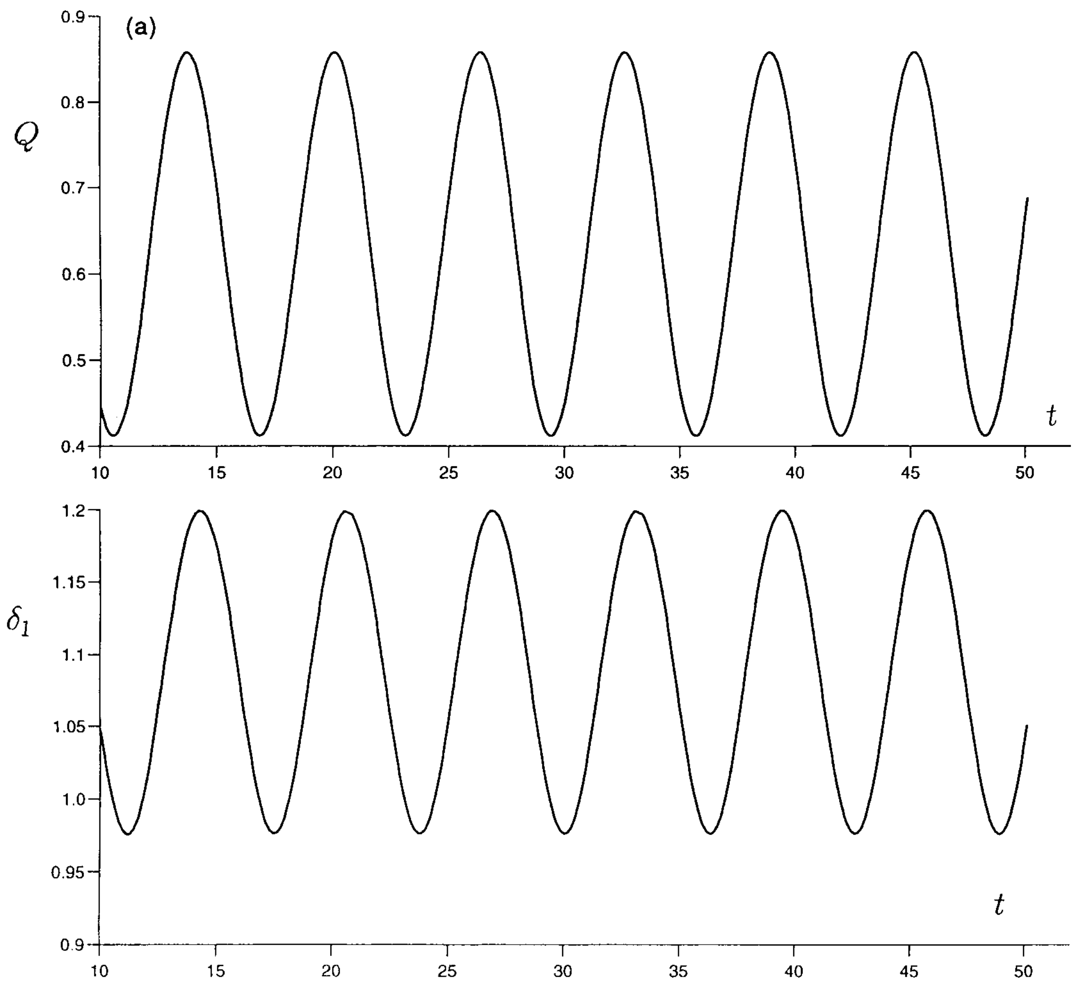

Fig. 1. Plots of heat transfer rate Q and boundary-layer thickness δ_1 against t obtained from numerical solutions of Eq. (13) subject to Eq. (14), plotted after the initial transients have died out, for (a) $A = 0.2$, $\omega = 1.0$; (b) $A = 0.4$, $\omega = 0.25$ and (c) $A = 0.5$, $\omega = 4.0$.

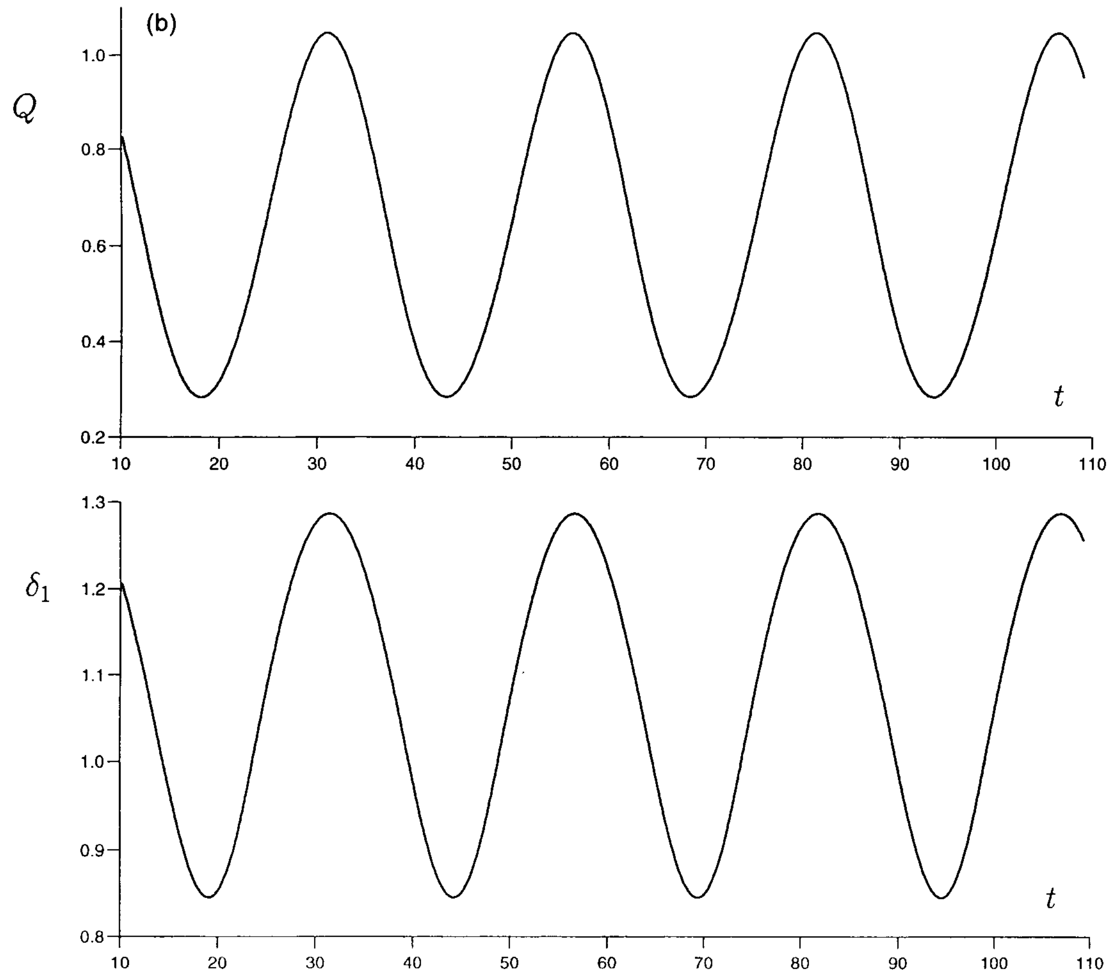

Fig. 1 (*continued*)

be gained from expansions for small amplitude ($A \ll 1$) and for fast ($\omega \gg 1$) and slow ($\omega \ll 1$) oscillations. We restrict our attention entirely to the large time behaviour, after all transients have died out, in these solutions. We find it more convenient to rescale t by writing $\tau = \omega t$, so that Eq. (13) becomes

$$\frac{\partial^3 f}{\partial y^3} + f\frac{\partial^2 f}{\partial y^2} = \omega \frac{\partial^2 f}{\partial y \, \partial \tau} \tag{17}$$

with boundary condition (14), on $y = 0$, becoming

$$\frac{\partial f}{\partial y} = 1 + A \sin \tau \tag{18}$$

We start by obtaining a solution valid for A small.

3.1. Small amplitude, $A \ll 1$

Boundary condition (18) suggests looking for a solution valid for $A \ll 1$ by expanding in the form

$$f(y, \tau) = f_0(y) + A\big(g_1(y)\sin \tau + h_1(y)\cos \tau\big) + \cdots \tag{19}$$

where f_0 satisfies

$$\begin{gathered} f_0''' + f_0 f_0'' = 0, \\ f_0(0) = 0, \quad f_0'(0) = 1, \quad f_0'(\infty) = 0 \end{gathered} \tag{20}$$

where primes denote differentiation with respect to y. Eq. (20) is a standard free convection boundary-layer problem [15] having $f_0''(0) = -0.62756$, $f_0(\infty) = 1.14277$.

The equations satisfied by g_1 and h_1 are linear, namely

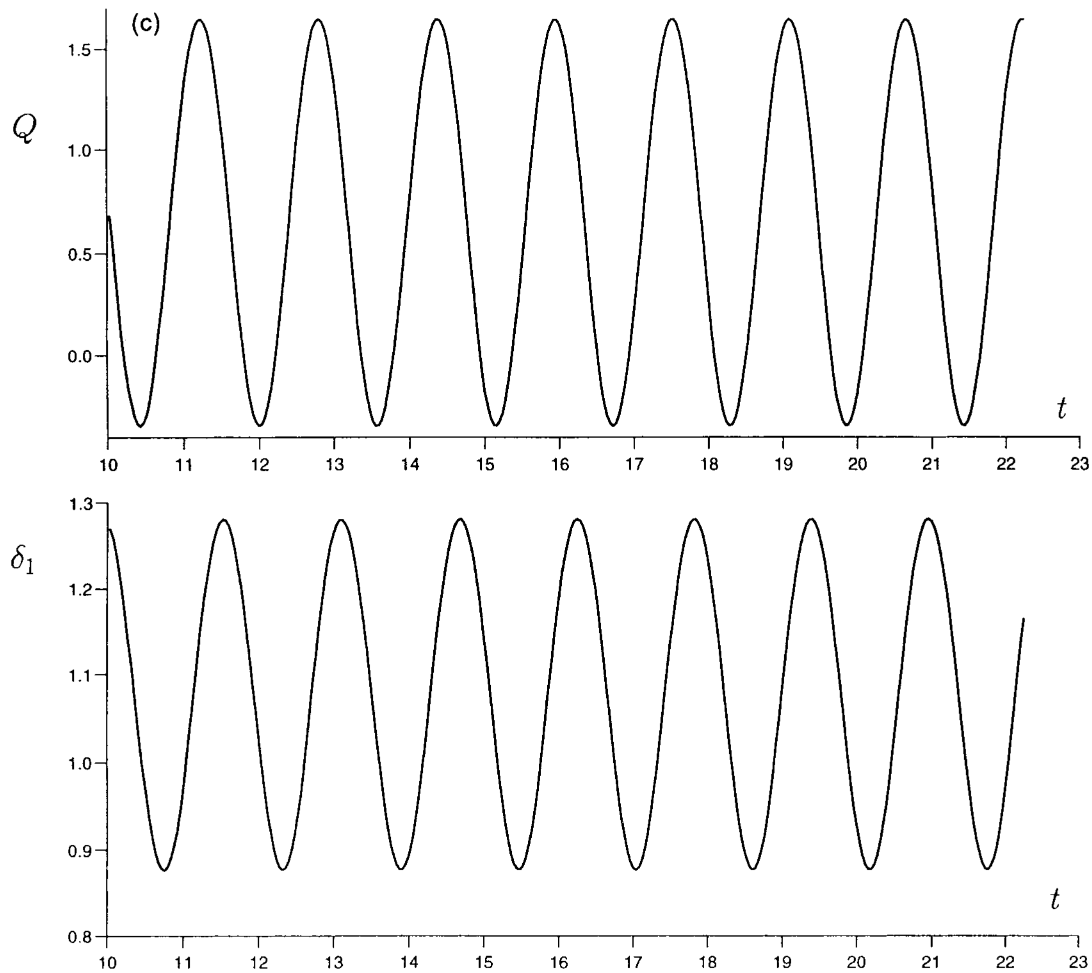

Fig. 1 (*continued*)

$$g_1''' + f_0 g_1'' + f_0'' g_1 = -\omega h_1'$$

$$h_1''' + f_0 h_1'' + f_0'' h_1 = \omega g_1' \tag{21}$$

subject to

$$g_1(0) = 0,\ g_1'(0) = 1,\ g_1'(\infty) = 0,$$
$$h_1(0) = 0,\ h_1'(0) = 0,\ h_1'(\infty) = 0 \tag{22}$$

Eqs. (21) and (22) have to be solved numerically. This is easily achieved using a standard boundary-value problem solver and the results (plots of $-g_1''(0)$ and $-h_1''(0)$ against ω) are shown in Fig. 2(a).

The terms at $O(A)$ are both oscillatory. These give rise, at $O(A^2)$, to oscillatory terms in $\sin 2\tau$ and $\cos 2\tau$ [9] as well as a further steady component $f_2(y)$, which satisfies

$$f_2''' + f_0 f_2'' + f_0'' f_2 = -\frac{1}{2}\left(g_1 g_1'' + h_1 h_1''\right)$$
$$f_2(0) = 0,\quad f_2'(0) = 0,\quad f_2'(\infty) = 0 \tag{23}$$

Eq. (23) can also be easily solved numerically and a graph of $f_2''(0)$ plotted against ω is shown in Fig. 2(b). This figure shows that $f_2''(0)$ is negative for all ω (and we find that $f_2(\infty)$ is also negative) in line with the results from the numerical integrations.

We can determine the behaviour of the solution of Eqs. (21) and (22), respectively, for both ω small and large. For small ω ($\ll 1$) the solution is regular, with

$$g_1(y) = G_0(y) + \omega^2 G_2(y) + \cdots,$$
$$h_1(y) = \omega H_1(y) + \cdots \tag{24}$$

where, on substituting Eq. (24) into Eq. (21) and

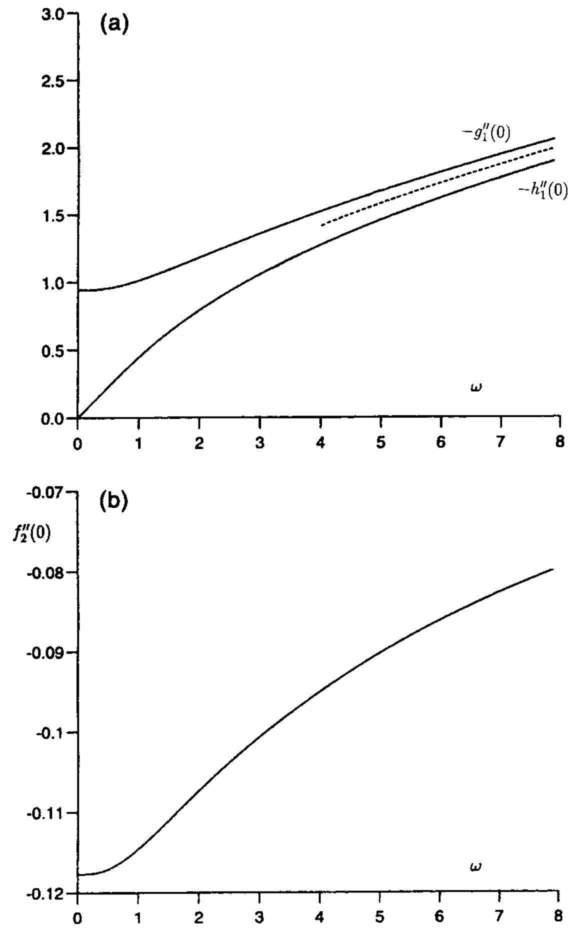

Fig. 2. (a) Plots of $-g_1''(0)$ and $h_1''(0)$ against ω obtained from the numerical solution of Eqs. (21) and (22). The asymptotic expression Eq. (29) for ω large is shown by the broken line. (b) A plot of $f_2''(0)$, the steady contribution at $O(A^2)$, obtained from the numerical solution of Eq. (23).

equating like powers of ω, we find that $G_0 = \frac{1}{2}(yf_0' + f_0)$, giving $G_0'''(0) = \frac{3}{2}f_0''(0) = -0.94133$, and then H_1 satisfies

$$H_1''' + f_0 H_1'' + f_0'' H_1 = \frac{1}{2}\left(yf_0'' + 2f_0'\right), \qquad H_1(0) = 0,\ H_1'(0) = 0,\ H_1'(\infty) = 0 \tag{25}$$

The numerical solution of this problem gives $H_1''(0) = -0.44434$. The form of solution for ω small given by Eqs. (24) and (25) can be seen in Fig. 2(a). The consequence of expansion (24) for f_2, the steady contribution at $O(A^2)$, is that, at leading order, f_2 satisfies Eq. (23) with the right-hand side replaced by $-\frac{1}{2}G_0G_0''$. The solution to this problem gives $f_2''(0) \sim -0.11767 + O(\omega^2)$ as $\omega \to 0$ in line with Fig. 2(b).

For large ω ($\gg 1$) the solution for g_1 and h_1 becomes confined to a thin region, of $O(\omega^{-1/2})$ thickness, in which we put

$$g_1 = \omega^{-1/2}\tilde{g}_1, \quad h_1 = \omega^{-1/2}\tilde{h}_1, \quad \tilde{y} = \omega^{1/2} y \tag{26}$$

We express f_0 as $f_0 \sim y - \frac{a_0}{2}y^2 + \cdots$ (where $a_0 = 0.62756$) and, with this, the substitution of Eq. (26) into Eq. (21) gives, at leading order,

$$\tilde{g}_1''' + \tilde{h}_1' = 0, \qquad \tilde{h}_1''' - \tilde{g}_1' = 0$$

$$\tilde{g}_1(0) = 0,\ \tilde{g}_1'(0) = 1,\ \tilde{g}_1'(\infty) = 0, \qquad \tilde{h}_1(0) = 0,\ \tilde{h}_1'(0) = 0,\ \tilde{h}_1'(\infty) = 0 \tag{27}$$

primes now denote differentiation with respect to $\tilde{y}$. The solution of Eq. (27) gives

$$\tilde{g}_1' = \exp\left(-\tilde{y}/\sqrt{2}\right)\cos\left(\tilde{y}/\sqrt{2}\right), \qquad \tilde{h}_1' = -\exp\left(-\tilde{y}/\sqrt{2}\right)\sin\left(\tilde{y}/\sqrt{2}\right) \tag{28}$$

from which we obtain

$$g_1''(0) \sim -\frac{\omega^{1/2}}{\sqrt{2}} + \cdots, \qquad h_1''(0) \sim -\frac{\omega^{1/2}}{\sqrt{2}} + \cdots \quad \text{as } \omega \to \infty \tag{29}$$

Expressions (29) are also shown in Fig. 2(a) (by the broken line). We note that, combining expressions (28) in expansion (19), gives the $O(A)$ term as

$$-\exp\left(-\tilde{y}/\sqrt{2}\right)\sin\left(\tilde{y}/\sqrt{2} - \tau\right) \quad \text{as } \omega \to \infty \tag{30}$$

The consequence of transformation (26) for f_2, as given by Eq. (23), is that f_2 is $O(\omega^{-3/2})$ for ω large. Putting $f_2 = \omega^{-3/2}\tilde{f}_2$, we find that $\tilde{f}_2$ satisfies the equation, on using Eqs. (27) and (28),

$$\tilde{f}_2''' = \frac{1}{2}\exp\left(-\tilde{y}/\sqrt{2}\right)\sin\left(\tilde{y}/\sqrt{2}\right) \tag{31}$$

Integrating this, with the condition that $\tilde{f}'(0) = 0$, gives

$$\tilde{f}_2' = -\frac{1}{2}\left(1 - \exp\left(-\tilde{y}/\sqrt{2}\right)\cos\left(\tilde{y}/\sqrt{2}\right)\right) \quad \text{with } \tilde{f}_2''(0) = -\frac{1}{2\sqrt{2}} \tag{32}$$

Hence $f_2''(0) \sim -\frac{\omega^{-1/2}}{2\sqrt{2}} + \cdots$ as $\omega \to \infty$.

Expression (32) for $\tilde{f}_2'$ does not satisfy the required outer boundary condition and a further outer region is needed to achieve this. We do into pursue this further at this stage but turn to looking for asymptotic solutions valid for ω both small and large with A of $O(1)$, where the details of this outer region will emerge.

3.2. ω small (slow oscillations)

The solution derived in the previous section for small ω suggests that, to obtain a solution of Eqs. (17) and (18) with A of $O(1)$ valid for $\omega \ll 1$, we should put

$$f = (1 + A\sin\tau)^{1/2} f_0(Y), \qquad Y = (1 + A\sin\tau)^{1/2} y \quad (33)$$

The substitution of Eq. (33) into Eqs. (17) and (18) gives, at leading order, the problem given by Eq. (20) for f_0 (now in terms of the transformed variable Y). From which it follows that

$$Q \sim 0.62756(1 + A\sin\tau)^{3/2} + \cdots,$$
$$\delta_1 \sim 1.1428(1 + A\sin\tau)^{1/2} + \cdots \quad \text{as } \omega \to 0 \quad (34)$$

We note that expression (34) agrees with the small A solution, as given by Eq. (19), to $O(A)$. Expressions (34) show that, for ω small at least, the response in both Q and δ_1 is oscillatory with the same frequency as the applied wall temperature (as borne out by the numerical integrations, see Fig. 1(b)). The amplitude of the response in Q, namely $0.62756((1+A)^{3/2} - (1-A)^{3/2})$, is generally larger, for a given A, than the amplitude of the oscillations in δ_1, namely $1.1428((1+A)^{1/2} - (1-A)^{1/2})$. We illustrate this with a specific example of $A = 0.4$ where these expressions for the amplitude give 0.7479 and 0.4670, respectively (compare with Fig. 1(b), for which the numerically computed values are, respectively, 0.763 and 0.442).

The solution for small ω, as given by Eqs. (33) and (34), holds only for $A < 1$. This puts a limit, in this parameter regime, for which a solution to Eq. (13) which satisfies boundary condition (14) for all t is possible. We examined the behaviour of the solution to this problem numerically, taking a small value for ω of $\omega = 0.1$ and a value for $A > 1$, namely $A = 1.4$. For these parameter values we were unable to keep satisfying the outer boundary condition as t increased with the numerical solution becoming unreliable after a finite time had elapsed (this time depend on the size of the computational domain). We illustrate the results in Fig. 3(a), where we show a temperature profile plot of $\theta = \partial f/\partial y$ at $t = 142$. This has an oscillatory region near the wall, as demonstrated by the plot of Q for this case shown in Fig. 3(b), and an increasingly large region where $\partial f/\partial y$ is negative and non-oscillatory. The numerical integrations for this (and cases where similar behaviour is seen) show that, when the wall temperature oscillates to negative values, this produces a steady and negative component in temperature $\theta = \partial f/\partial y$ a small distance from the wall. This then gives rise to a very rapidly increasing region where $\partial f/\partial y \neq 0$ to give temperature profiles like those shown in Fig. 3(a). This is not the case when $A < 1$, where the outer boundary condition can be satisfied with sufficient accuracy in the computations for very large values of t. We discuss this aspect more later, but now we turn to obtain a solution valid for large ω.

3.3. ω large (fast oscillations)

The solution for ω large and A small described above suggests that, to obtain a solution to Eqs. (17) and (18) valid for ω large and for general values of A, we should start in a thin inner region of thickness $O(\omega^{-1/2})$ in which we put

$$f = \omega^{-1/2} F, \qquad \tilde{y} = \omega^{1/2} y \quad (35)$$

Transformation (35) applied to Eq. (17) leads to

$$\frac{\partial^3 F}{\partial \tilde{y}^3} - \frac{\partial^2 F}{\partial \tilde{y}\,\partial \tau} = -\omega^{-1} F \frac{\partial^2 F}{\partial \tilde{y}^2}$$
$$\text{with } \frac{\partial F}{\partial \tilde{y}} = 1 + A\sin\tau \text{ on } \tilde{y} = 0 \quad (36)$$

The form of the boundary condition suggests that the solution is, at leading order,

$$F_0(\tilde{y}, \tau) = \tilde{F}_0(\tilde{y}) + A\Big(\tilde{g}_1(\tilde{y})\sin\tau + \tilde{h}_1(\tilde{y})\cos\tau\Big) \quad (37)$$

where $\tilde{F}_0 = \tilde{y}$ and where $\tilde{g}_1$ and $\tilde{h}_1$ have been given already in Eq. (28).

The outer solution described below leads to a steady $O(\omega^{-1/2})$ contribution $\tilde{F}_1 = -a_0\frac{\tilde{y}^2}{2}$ in the inner region. At $O(\omega^{-1})$ we have oscillatory contributions in $\sin 2\tau$ and $\cos 2\tau$ as well as a steady contribution given by

$$\tilde{F}_2' = -\frac{A^2}{2}\big(1 - \exp(-\tilde{y}/\sqrt{2})\cos(\tilde{y}/\sqrt{2})\big) \quad (38)$$

Expression (38) gives a contribution of $\frac{A^2}{2\sqrt{2}}\omega^{-1/2}$ to the mean in the oscillations of Q, and from Eqs. (28), (35) and (37) we have

$$Q \sim \omega^{1/2} A \sin\left(\tau + \frac{\pi}{4}\right) + a_0 + \cdots \quad \text{as } \omega \to \infty \quad (39)$$

At the outer edge of the inner region we have, from Eqs. (37) and(38), that

$$f \sim y - \frac{a_0}{2} y^2 + \cdots + \omega^{-1}\left(-\frac{A^2}{2} y + \cdots\right) + \cdots \quad (40)$$

This suggests looking for a steady solution to Eqs. (17) and (18) in the form

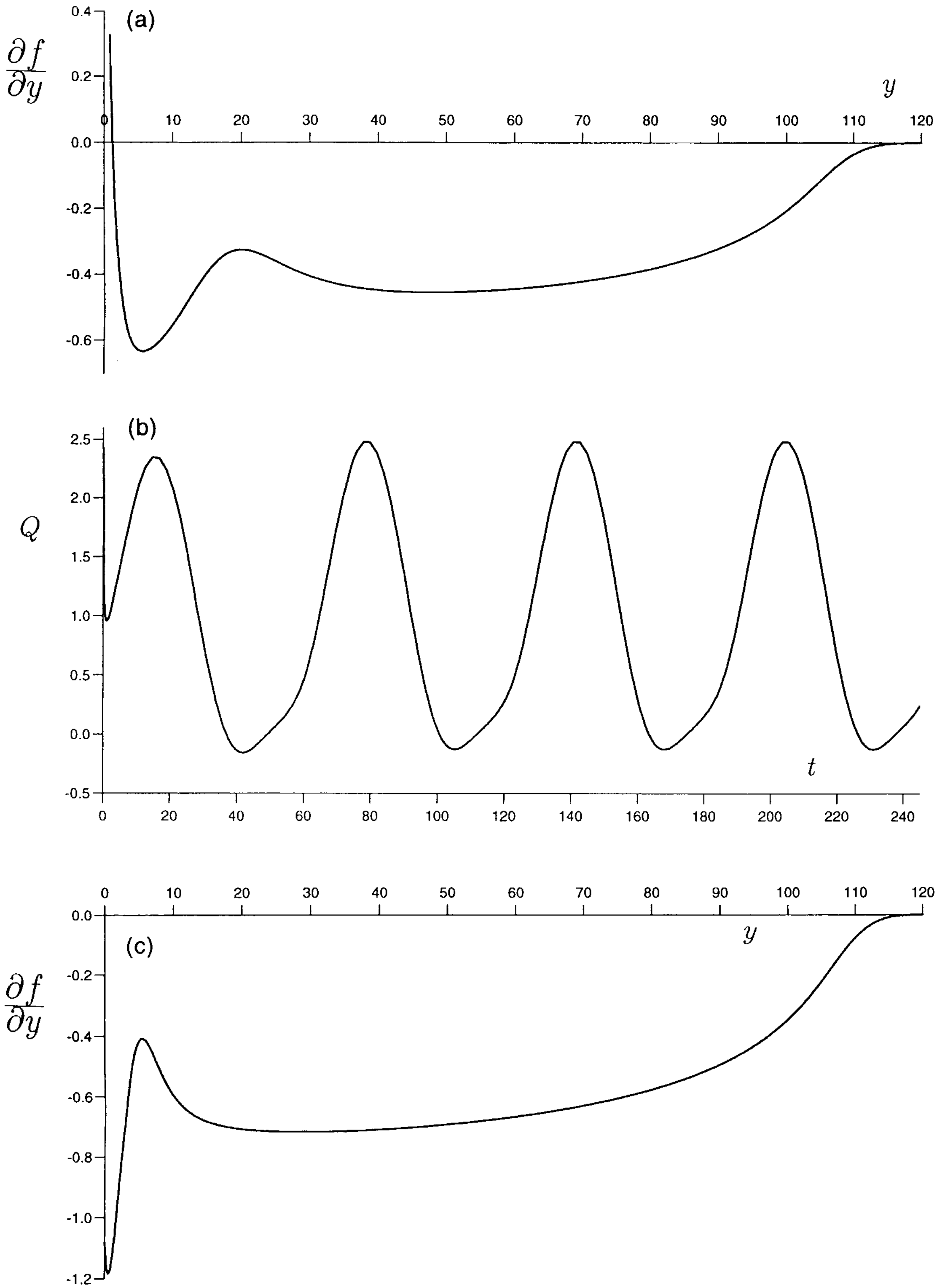

Fig. 3. (a) A plot of the temperature profile $\theta = \partial f/\partial y$ at $t = 142$ for $A = 1.2$, $\omega = 0.1$ obtained from the numerical integration of Eqs. (13) and (14); (b) a plot of Q against t for the above parameter values; (c) a profile plot of $\theta = \partial f/\partial y$ at $t = 11.6$ for $A = 2.5$, $\omega = 1.0$.

$$f(y) = f_0(y) + \omega^{-1} f_1(y) + \cdots \tag{41}$$

where f_0 satisfies (20) and where $f_1 = -\frac{A^2}{4}(yf_0' + f_0)$. From Eqs. (35), (37) and (41) we then have

$$\delta_1 \sim 1.1428 + \omega^{-1/2} A \sin\left(\tau - \frac{\pi}{4}\right) + \cdots \quad \text{as } \omega \to \infty \tag{42}$$

3.4. Large amplitude, $A \gg 1$

The numerical integrations show that there is a value $A_{\max}$ of A such that solutions to initial-value problem (Eqs. (13) and (14)) which are bounded for all t do not exist for $A > A_{\max}$ (see Fig. 3(a)). $A_{\max}$ depends on ω and we have been able to establish that $A_{\max} \to 1$ as $\omega \to 0$. The numerical integrations show that $A_{\max}$ increases with ω and the large ω analysis does not provide an obvious upper bound on A. We have already shown these unbounded solutions for ω small (Fig. 3(a),(b)) and illustrate their dependence on ω for the further case of $\omega = 1.0$, taking $A = 2.5$. A temperature profile plot of $\theta = \partial f/\partial y$ for this case is shown in Fig. 3(c). For $\omega = 1.0$ we find bounded solutions for all A up to $A = 1.95$ but not for $A = 2.0$.

Bounded solutions are possible for A large provided ω is also large, of $O(A^2)$. If we put $\omega = \omega_0 A^2$, where ω_0 is of $O(1)$, and then $\tilde{Y} = Ay$ (leaving f unscaled) we arrive at the leading order problem for A large

$$\frac{\partial^3 f}{\partial \tilde{Y}^3} = \omega_0 \frac{\partial^2 f}{\partial \tilde{Y} \partial \tau}, \quad \frac{\partial f}{\partial \tilde{Y}} = \sin\tau \ \text{ on } \ \tilde{Y} = 0 \tag{43}$$

The solution to Eq. (43) is standard

$$\frac{\partial f}{\partial \tilde{Y}} = -\exp\left(-\sqrt{\frac{\omega_0}{2}}\tilde{Y}\right)\sin\left(\sqrt{\frac{\omega_0}{2}}\tilde{Y} - \tau\right) \tag{44}$$

giving

$$\begin{aligned} Q &\sim A^2\sqrt{\omega_0}\,\sin\left(\tau + \frac{\pi}{4}\right) + \cdots \\ &= \omega^{1/2} A \sin\left(\tau + \frac{\pi}{4}\right) + \cdots \\ &\text{as } A \to \infty \end{aligned} \tag{45}$$

with ω of $O(A^2)$, which compares directly with expression (39) derived only on the assumption that ω was large.

If we now take ω to be only of $O(A)$, i.e., we put $\omega = \omega_1 A$, and then scale $f = A^{1/2}\hat{F}$, $\hat{Y} = A^{1/2} y$, we obtain, at leading order, the problem given by Eq. (17) with ω replaced by ω_1, and now subject to, at leading order, $\partial\hat{F}/\partial\hat{Y} = \sin\tau$ on $\hat{Y} = 0$. A bounded solution to this problem, valid for ω_1, large, can be obtained essentially in the same form as for the ω large solution given above (see Eqs. (26)–(28), (36) and (37)), and we get

$$Q \sim A^{3/2}\omega_1^{1/2}\sin\left(\tau + \frac{\pi}{4}\right) + \ldots \quad \text{as } \omega_1 \to \infty,\ \omega \text{ of } O(A) \tag{46}$$

In this limit Eq. (46) agrees with (45). However, numerical solutions to the problem show that a bounded solution does not exist for all ω_1 with there being a lower bound on ω_1 for the existence of such solutions. This suggests that $A_{\max}$ is of $O(\omega)$ for ω large.

The main feature of the solution for $A > A_{\max}$ is that the oscillations in the wall temperature generate a steady (negative) response in the stream function f so that, after a relatively few oscillations, $f \sim -\gamma y$, for some positive constant γ which will depend on ω and A, at the edge of the oscillatory region. This then acts to set up a rapidly growing outer region in which the stream function f is non-oscillatory. A further consideration of this region shows that its behaviour is strictly analogous to the boundary-layer collision region at the top of a horizontal cylinder described in detail by Ingham et al. [16]. The details are essentially the same (apart from an obvious scaling factor) and need not be repeated. The main features are that the thickness of the boundary layer grows at an exponential, $O(e^{\gamma t})$ rate behind a propagating front structure which spreads at an $O(t^{1/2})$ rate. This effect can be seen as the numerical solutions evolve and is suggested by the profile plots in Fig. 3(a) and (c).

4. Conclusion

The problem of unsteady free convection boundary-layer flow near a stagnation-point of a two-dimensional cylindrical surface in a porous medium has been studied when the surface temperature oscillates around a mean value T_w above ambient. Since non-uniform surface temperature variations are more likely to occur in practice than uniform conditions, it is important to determine the extent to which these non-uniformities affect the boundary-layer responses. In order to gain some insight into the basic heat transfer mechanism, numerical and asymptotic solutions of the governing equations have been obtained for both small and large values of the amplitude parameter A and for both slow and fast oscillations, i.e. small and large values of the frequency parameter ω. For small amplitude oscillations ($A \ll 1$), the response remains small, of $O(A)$, and oscillatory with the same frequency of the oscillations in the surface temperature, though a small phase shift is seen. This is, perhaps, to be expected from previous studies [10,11].

For fast oscillations (ω large) there is still an oscillatory response (at the same frequency as the surface temperature) but now this is confined to a thin region close to the wall. In this case the oscillations in surface temperature set up a steady outer flow, though still remaining within the overall boundary-layer region. For slow oscillations (ω small), it was seen that the response in heat transfer rate Q and boundary-layer thickness δ_1 is also oscillatory with the same frequency as the applied wall temperature distribution when $A < 1$. However, for $A > 1$ the numerical results show that, while the solution near the wall remains oscillatory, a region develops in which there is a steady temperature below ambient and which propagates rapidly away from the wall. This leads to the general conclusion that there is a value $A_{\max}$ of A such that solutions to the governing equations, which are bounded for all times, do not exist when $A > A_{\max}$. We have shown that $A_{\max} \to 1$ as $\omega \to 0$ and that $A_{\max}$ increases with ω with the $\omega \gg 1$ analysis not providing an obvious upper bound on A. A more detailed consideration of the solutions for $A > A_{\max}$ shows that the oscillation in the surface temperature generates a steady (negative) flow region that is similar to the transient free convection boundary-layer region at the top of a horizontal cylinder embedded in a porous medium which is impulsively heated, as described by Ingham et al. [16].

The practical importance of the present study is that it presents for the first time means of estimating the heat transfer rate from a surface whose temperature oscillates in time and which is embedded in a porous medium. It is hoped that experimental data of this new type of driven convective flow in porous media will become available in the future to justify the present theoretical results.

References

[1] A. Bejan, Convective heat transfer in porous media, in: S. Kakac, R.K. Shah, W. Aung (Eds.), Handbook of Single-Phase Convective Heat Transfer, Wiley, New York, 1987 (Sections 16.1–16.34).

[2] A. Nakayama, PC-Aided Numerical Heat Transfer and Convective Flow, CRC Press, Tokyo, 1995.

[3] S. Kimura, T. Kiwata, A. Okajima, I. Pop, Conjugate natural convection in porous media, Advances in Water Research; Special Issue: Advances in Heat Transfer in Porous Media 20 (1997) 111–126.

[4] D.A. Nield, A. Bejan, Convection in Porous Media, 2nd ed., Springer-Verlag, New York, 1999.

[5] D.B. Ingham, I. Pop, Transport Phenomena in Porous Media, Pergamon Press, Oxford, 1998.

[6] B.J. Minto, D.B. Ingham, I. Pop, Free convection driven by an exothermic reaction on a vertical surface embedded in porous media, International Journal of Heat and Mass Transfer 41 (1998) 11–23.

[7] J.H. Merkin, T. Mahmood, Convective flows on reactive surfaces in porous media, Transport in Porous Media 33 (1998) 279–293.

[8] T. Mahmood, J.H. Merkin, The convective boundary-layer flow on a reacting surface in a porous medium, Transport in Porous Media 32 (1998) 285–298.

[9] J.H. Merkin, Oscillatory free convection from an infinite horizontal cylinder, Journal of Fluid Mechanics 30 (1967) 561–575.

[10] M.D. Kelleher, K.-Y. Yang, Heat transfer response of laminar free-convection boundary layers along a vertical heated plate to surface-temperature oscillations, Journal of Applied Mathematics and Physics (ZAMP) 19 (1968) 31–44.

[11] S.N. Brown, N. Riley, Propagation of disturbances in an unsteady free-convection boundary layer, Journal of Applied Mathematics and Physics (ZAMP) 25 (1974) 145–156.

[12] I. Pop, D.B. Ingham, J.H. Merkin, Transient convection heat transfer in a porous medium: external flows, in: D.B. Ingham, I. Pop (Eds.), Transport Phenomena in Porous Media, Pergamon Press, Oxford, 1998, pp. 205–231.

[13] M.A. Chaudhary, J.H. Merkin, Free convection stagnation point boundary layers driven by catalytic surface reactions. Part I: The steady states, Journal of Engineering Mathematics 28 (1994) 145–171.

[14] M.A. Chaudhary, J.H. Merkin, Free convection stagnation point boundary layers driven by catalytic surface reactions. Part II: Times to ignition, Journal of Engineering Mathematics 30 (1996) 403–415.

[15] J.H. Merkin, Free convection boundary layers on axisymmetric and two-dimensional bodies of arbitrary shape in a saturated porous medium, International Journal of Heat and Mass Transfer 22 (1979) 1461–1462.

[16] D.B. Ingham, J.H. Merkin, I. Pop, The collision of free-convection boundary layers on a horizontal cylinder in a porous medium, Quarterly Journal of Mechanics and Applied Mathematics 36 (1983) 313–335.